Check for updates

European Journal of Immunology Clinical·Basic·Translational

Allergy and inflammation

Clinical

Short Communication

Predominance of M2 macrophages in organized thrombi in chronic thromboembolic pulmonary hypertension patients

Thomas Koudstaal[1], Thierry van den Bosch[2], Ingrid Bergen[1], Karishma Lila[2], Paul Bresser[3], Harm Jan Bogaard[4], Karin Boomars[1], Rudi Hendriks[#1] and Jan von der Thüsen[#2]

[1] Department of Pulmonary Medicine, Erasmus MC, University Medical Center Rotterdam, Rotterdam, the Netherlands
[2] Department of Pathology and Clinical Bioinformatics, Erasmus MC, University Medical Center Rotterdam, Rotterdam, the Netherlands
[3] Department of Pulmonary Medicine, Onze Lieve Vrouwe Gasthuis, Amsterdam, the Netherlands
[4] Department of Pulmonary Medicine, VU Medical Centre, Amsterdam, the Netherlands

Chronic thromboembolic pulmonary hypertension **(CTEPH) is a debilitating disease characterized by thrombotic occlusion of pulmonary arteries and vasculopathy, leading to increased pulmonary vascular resistance and progressive right-sided heart failure. Thrombotic lesions in CTEPH contain CD68$^+$ macrophages, and increasing evidence supports their role in disease pathogenesis. Macrophages are classically divided into pro-inflammatory M1 macrophages and anti-inflammatory M2 macrophages, which are involved in wound healing and tissue repair. Currently, the phenotype of macrophages and their localization within thrombotic lesions of CTEPH are largely unknown. In our study, we subclassified thrombotic lesions of CTEPH patients into developing fresh thrombi (FT) and organized thrombi (OT), based on the degree of fibrosis and remodeling. We used multiplex immunofluorescence histology to identify immune cell infiltrates in thrombotic lesions of CPTEH patients. Utilizing software-assisted cell detection and quantification, increased proportions of macrophages were observed in immune cell infiltrates of OT lesions, compared with FT. Strikingly, the proportions with a CD206$^+$INOS$^-$ M2 phenotype were significantly higher in OT than in FT, which mainly contained unpolarized macrophages. Taken together, we observed a shift from unpolarized macrophages in FT toward an expanded population of M2 macrophages in OT, indicating a dynamic role of macrophages during CTEPH pathogenesis.**

Keywords: Chronic thromboembolic pulmonary hypertension · Inflammation and immunity · Macrophages

Additional supporting information may be found online in the Supporting Information section at the end of the article.

Introduction

Chronic thromboembolic pulmonary hypertension (CTEPH) is a devastating cardiopulmonary disease resulting from a rare complication following acute pulmonary embolism [1], leading to increased pulmonary vascular resistance and progressive right-heart failure. Depending on the localization and characterization of the thrombotic lesions in the pulmonary vasculature, current therapies include pulmonary endarterectomy (PEA) surgery, balloon pulmonary angioplasty (BPA) intervention, and/or pulmonary hypertension (PH)-specific drug therapy. Hereby, PEA and BPA lead to good long-term survival for most eligible patients [2]. Patients with CTEPH who have thrombotic lesions mainly in the periphery or significant co-morbidities are inoperable and have a poor prognosis, with a mean 5-year survival of 53–69% even with specific PH medication [2]. Therefore,

Correspondence: Dr. Thomas Koudstaal
e-mail: t.koudstaal.1@erasmusmc.nl

[#]Rudi Hendriks and Jan von der Thüsen shared the last authorship.

© 2024 The Authors. *European Journal of Immunology* published by Wiley-VCH GmbH.

This is an open access article under the terms of the Creative Commons Attribution-NonCommercial-NoDerivs License, which permits use and distribution in any medium, provided the original work is properly cited, the use is non-commercial and no modifications or adaptations are made.

more insight into the pathogenesis of CTEPH is urgently needed and could fuel the development of new therapeutic strategies.

Thrombotic lesions of CTEPH patients contain various immune cells, particularly myeloid cells including macrophages [2, 3]. Interestingly, in an analysis of serum from eight CTEPH patients, increased concentrations of monocyte chemoattractant protein-1 (MCP-1, CCL2) and macrophage inflammatory protein-1α (MIP-1α/CCL3) were detected [4]. These chemokines have the capacity to induce chemotactic mobilization of myeloid cells, resulting in the recruitment of macrophages, local synthesis of inflammatory cytokines, and vascular remodeling. Macrophages are classified into M1 proinflammatory and M2 anti-inflammatory subtypes [5]. Whereas M1 macrophages are responsible for initiating and sustaining inflammation, M2 macrophages — which are also referred to as alternatively activated macrophages — [5] participate in the resolution of inflammation, wound healing, and tissue repair. Recent single-cell RNA sequencing (scRNAseq) and lineage-tracing studies have defined multiple additional pulmonary macrophage subtypes in humans and mice, beyond the M1/M2 classification [6–8]. For example, Takiguchi et al. found that CD40/CD163 double-negative macrophages in bronchoalveolar lavage fluid expressed a proinflammatory gene signature [8].

An imbalance of M1 and M2 macrophages has been implicated in the development of tumors, obesity, osteoarthritis, and atherosclerosis [9]. A recent study revealed that macrophage depletion in mice results in experimental pulmonary hypertension and an altered M1/M2 ratio in the lung [10], suggesting a significant modifying role of macrophages in the pathogenesis of CTEPH. Previous research has demonstrated an increase in CD206+CD68+ cells with an M2 phenotype in CTEPH thrombotic lesions [3], but a detailed quantification of M1, M2, double negative (DN), and double positive (DP) macrophages is still lacking as earlier studies did not include markers for M1 macrophages and DP macrophages.

In this report, we utilized multiplex immunofluorescence to perform an in-depth subclassification of macrophages and T cells and used software-assisted cell detection to localize and quantify M1, M2, DN, and DP macrophages in thrombotic lesions from CTEPH patients.

Results and discussion

PEA samples from CTEPH patients contain immune infiltrates with distinct macrophage subpopulations

To identify the presence of immune infiltrates in paraffin-embedded vascular lesions of 23 CTEPH patients, we compared serial sections of H&E staining and multiplex immunofluorescence. Dense lymphocytic infiltrates were visible in thrombotic lesions from 18 CTEPH patients. In the remaining 5 CTEPH PEA samples, cellular infiltration was detected, but immune cells were more randomly distributed.

CTEPH thrombotic lesions were classified histologically into two categories: developing fresh thrombi (FT; $n = 6$) and completely organized thrombi (OT; $n = 12$) (Fig. 1A and B).

Developing FT refers to growing thrombi with at least a partial presence of recently formed blood clots that have not yet undergone significant organization or remodeling. These clots are composed of platelets, fibrin, erythrocytes, and lymphocytes, and may co-exist with adjacent areas of organized thrombus. On the other hand, OT refers to older thrombi that have undergone complete remodeling and are characterized by the presence of fibrous tissue, neovascularization, and recanalization, without any histological evidence of recent thrombosis.

We identified $CD31^+$ vascular endothelial cells and used inducible nitric oxide synthase (iNOS) and the mannose receptor CD206 to detect the presence of $INOS^+CD68^+$ M1 macrophages and $CD206^+CD68^+$ M2 macrophages, respectively (Fig. 1A and B). While the number of CD31+ cells is expected to be similar between the FT and OT groups, it is important to note that the distribution of CD31+ cells may vary between small and large arterioles within the thrombi. This difference in distribution suggests that the vascularization patterns in FT and OT will be distinct. In FT, where the thrombus is relatively fresh and less organized, we anticipate observing a more scattered distribution of CD31+ cells in the small arterioles. In contrast, in OT where the thrombus has undergone remodeling, we expect to see a more organized and structured distribution of CD31+ cells in both small and large arterioles.

In our previous work, we demonstrated an increased accumulation of $CCR6^+$ T cells in OT compared with FT in CTEPH [11], potentially due to chemokine CCL20, which is known to interact only with CCR6 [12]. In OT this may have attracted $CCR6^+$ cells, including Th17 cells known for their involvement in autoimmunity [13].

Next, Qupath software-assisted cell recognition and quantification was used to determine the presence and proportions of T cells, M1 and M2 macrophages in 18 out of 23 thrombotic lesions. After careful evaluation and demarcation of the regions of infiltration, using adjacent serial H&E sections, borders around the infiltrates were manually defined. Within the demarcated areas, automated cell detection was performed based on nuclear staining with 4′,6-diamidino-2-phenylindole (DAPI) and $CD3^+$ T cells, $INOS^+CD68^+$ M1 and $CD206^+CD68^+$ M2 macrophages, as well as $CD206^+INOS^+$ DP and unpolarized DN $CD68^+$ $INOS^-$ $CD206^-$ (DN) macrophages were identified (Fig. 1C and D). To further support that $CD68^+$ $CD206^+$ macrophages exhibit an M2 orientation, we conducted additional 5-plex-immunofluorescent staining to detect M2-associated markers, including Arginase, IL10, and TGF-β in representative vascular lesions of a subgroup of 6 CTEPH patients (Table 1, Supporting information Fig. 1A). The results of these stainings demonstrated that >98% of $CD68^+$ $CD206^+$ macrophages tested positive for 1 or more of these additional M2 markers, thereby supporting their M2 phenotype (Supporting information Fig. 1B).

The identification of four individual macrophage subpopulations parallels reported findings in broncho-alveolar-lavage

© 2024 The Authors. European Journal of Immunology published by Wiley-VCH GmbH.

15214141, 2024, 6, Downloaded from https://onlinelibrary.wiley.com/doi/10.1002/eji.202350670 by Erasmus University Rotterdam Universiteitsbibliotheek, Wiley Online Library on [12/06/2024]. See the Terms and Conditions (https://onlinelibrary.wiley.com/terms-and-conditions) on Wiley Online Library for rules of use; OA articles are governed by the applicable Creative Commons License

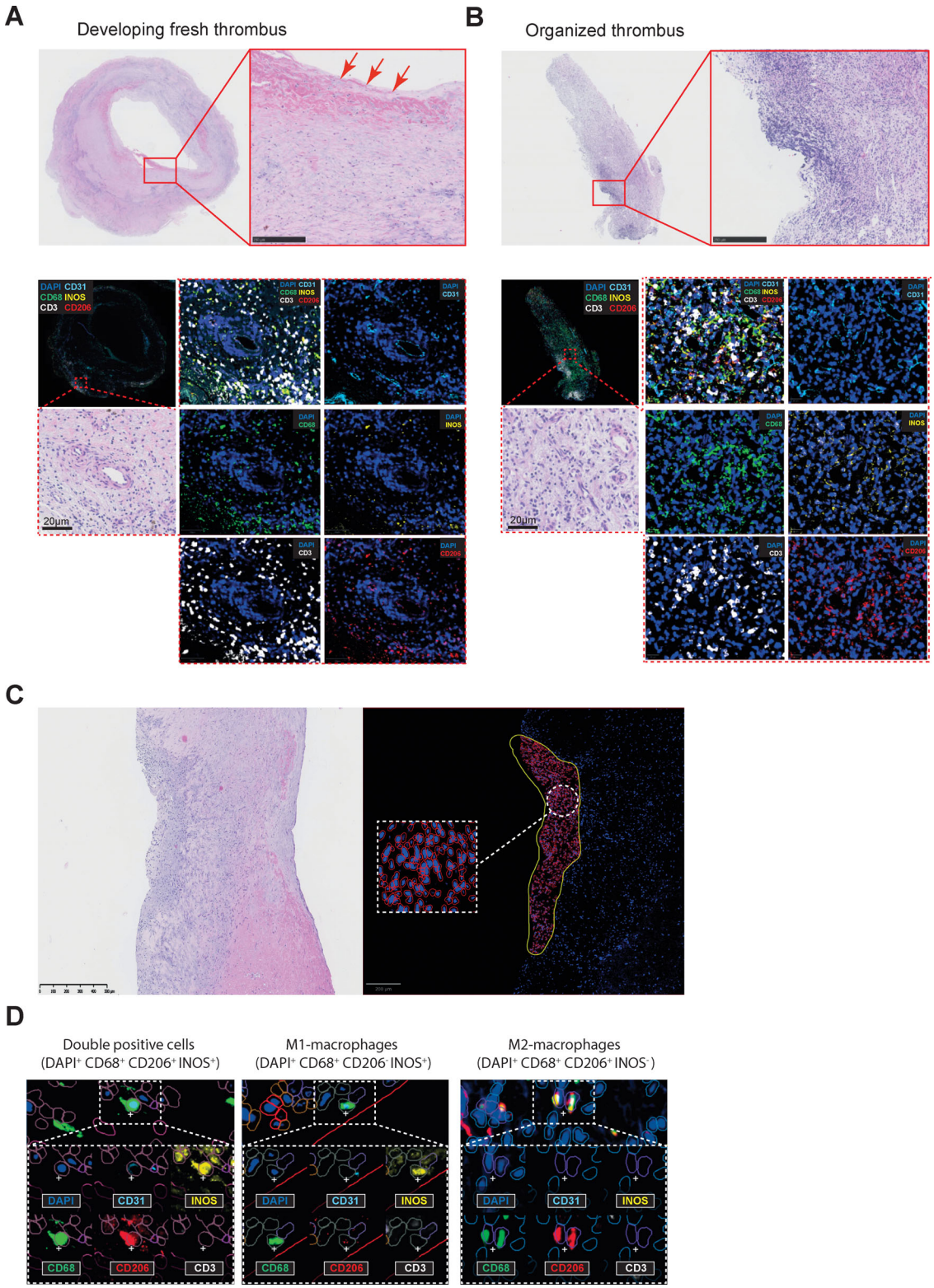

Figure 1. Vascular lesions of CTEPH patients contain immune infiltrates with distinct macrophage subpopulations. Representative samples are shown for developing fresh (A) and organized (B) thrombi in CTEPH patients. Panels display H&E staining (top panel, bottom left) and the corresponding 5-plex-immunofluorescent staining of INOS (yellow), CD4 (red), CD68 (green), CD31 (aqua), CD3 (white), and DAPI (blue) in two representative vascular lesions of CTEPH patients. Magnification of the indicated area (bottom left and middle and right panels) for immunofluorescent multiplex staining of a vascular lesion containing $CD3^+$ T cells, $CD68^+INOS^+$ M1 macrophages, and $CD68^+CD206^+$ M2 macrophages near $CD31^+$ vasculature. Scale in overview is 100 µm and in high magnifications 20 µm both in H&E and multiplex immunofluorescence staining images. Red arrows in the top left indicate fresh thrombotic material. (C) Analysis of the multiplex staining was performed using Qupath, an open software platform for bioim-

© 2024 The Authors. *European Journal of Immunology* published by Wiley-VCH GmbH.

15214141, 2024, 6, Downloaded from https://onlinelibrary.wiley.com/doi/10.1002/eji.202350670 by Erasmus University Rotterdam Universiteitsbibliotheek, Wiley Online Library on [12/06/2024]. See the Terms and Conditions (https://onlinelibrary.wiley.com/terms-and-conditions) on Wiley Online Library for rules of use; OA articles are governed by the applicable Creative Commons License

15214141, 2024, 6, Downloaded from https://onlinelibrary.wiley.com/doi/10.1002/eji.202350670 by Erasmus University Rotterdam Universiteitsbibliotheek, Wiley Online Library on [12/06/2024]. See the Terms and Conditions (https://onlinelibrary.wiley.com/terms-and-conditions) on Wiley Online Library for rules of use; OA articles are governed by the applicable Creative Commons License

Table 1. Patient characteristics.

	CTEPH lesions with organized thrombi (main study $n = 12$)	CTEPH lesions with organized thrombi (M2 markers substudy ($n = 3$)	CPTEH lesions with developing fresh thrombi (main study, $n = 11$)	CTEPH lesions with developing fresh thrombi (M2 markers substudy $n = 3$)	p value (for main study cohort)
Baseline clinical characteristics					
Gender, female n (%)	8 (67%)	2 (67%)	8 (73%)	1 (33%)	0.77
Age, years	49.2 ± 12.0	38.0 ± 18.3	54.9 ± 10.5	54.6 ± 6.5	0.25
BMI (kg/m^2)	28.6 ± 6.4	29.0 ± 9.1	31.5 ± 4.1	27.0 ± 5.4	0.22
NYHA class 3–4 (%)	4 (33%)	1 (33%)	9 (82%)	2 (67%)	0.02
NTproBNP (pmol/L)	25 ± 42	31 ± 33	49 ± 67	57 ± 44	0.46
Baseline right heart catheterization					
mPAP,mmHg	36.5 ± 21.3	33.7 ±26.3	39.2 ± 18.4	33.7 ± 17	0.75
Cappillary wedge pressure, mmHg	8.2 ± 3.8	8.7 ± 3.2	9.4 ± 3.7	8.3 ± 3.1	0.46
PVR, dynes/s/cm^{-5}	610.4 ± 631.5	359.5 ± 408.3	654.9 ± 562.6	434.4 ± 390.9	0.86
PH-medication					
At t = sample collection					
No PH-medication, n (%)	12 (100%)	3 (100%)	11 (100%)	3 (100%)	
Immunomodulatory drugs					
At sample collection, n (%)	12 (100%)	3 (100%)	11 (100%)	3 (100%)	

Note: p-values were calculated by nonparametric Mann–Whitney U test.
Abbreviations: BMI, body mass index; CTEPH, chronic thromboembolic pulmonary hypertension; 6MWT, 6-minute walk test; NT-pro BNP, The N-terminal prohormone of brain natriuretic peptide; mPAP, mean pulmonary arterial pressure; NYHA, New York Heart Association; PVR, pulmonary vascular resistance.

fluid and lungs of COPD patients [8, 14]. Previous research in atherosclerosis and stroke also demonstrated differences in cell infiltration between fresh and organized thrombi [15]. However, atherosclerotic plaques contained M1 macrophages in the plaque shoulder, while M2 macrophages were localized in the adventitia and areas of neovascularization [16]. In CTEPH, we did not see specific M1 or M2 zones in thrombotic lesions, but rather an overall increase in M2 macrophages in OT and a larger proportion of unpolarized DN macrophages in FT. Therefore, the macrophage compartment may be more dynamic and heterogeneous in CTEPH, compared with atherosclerotic plaques.

Major fractions of unpolarized macrophages in fresh thrombi and M2 macrophages in organized thrombi

Quantitative analysis of the selected areas of immune infiltration revealed that overall cell density and proportions of T cells and endothelial cells were variable, but did not differ between FT and OT (Fig. 2A). In contrast, we observed a striking proportional increase in macrophages within the immune infiltrates in OT, compared with the FT (Fig. 2B). Moreover, the proportions of CD206$^+$INOS$^-$CD68$^+$ M2 macrophages within the infiltrates were significantly higher in OT than in FT, while proportions of CD206$^-$INOS$^+$CD68$^+$ M1 macrophages were similar (Fig. 2C and D). Compared with OT, the relative frequency of DN cells in the macrophage population was increased in FT, indicating limited macrophage polarization. However, it cannot be excluded that the CD206$^+$INOS$^-$ DN fraction may contain proinflammatory macrophages, given that macrophage fractions in bronchoalveolar lavage that lack the M1 marker CD40 and the M2 marker CD163 were reported to have a proinflammatory gene signature [8]. Moreover, the impaired function of nonpolarized macrophages has been implicated in various lung diseases such as COPD, asthma, and fibrosis [18–21]. Nevertheless, we observed a substantial shift from DN macrophages in FT toward an expanded population of M2 macrophages in OT.

It remains unclear whether macrophages in thrombotic lesions play a mainly pathological or protective role, or are rather bystander cells following pulmonary embolism. The increased prevalence of M2 macrophages in OT is noteworthy, as they have been found to have regulatory properties with increased IL-10 production, similar to their abundance in murine models for

age analysis (version 0.3.0) [17]. Serial sections were evaluated for infiltration of immune cells by H&E staining according to standard procedures and subsequently annotated using specific thresholds for cell detection. The thresholds for automated 4′,6-diamidino-2-phenylindole (DAPI)-based cell detection were determined on the basis of comparisons between manual H&E and automated DAPI quantifications in paired slides. Afterward, using thresholding for the different channels, all cells were automatically classified and annotated based on specific clusters of markers. Scale in H&E and corresponding immunofluorescence 5-plex staining overview is 20 µm. (D) Determination of the proportions of M1 (CD68$^+$INOS$^+$), M2 (CD68$^+$CD206$^+$), and double positive (CD68$^+$INOS$^+$CD206$^+$) macrophages within the indicated CD68$^+$ subpopulations. Quantifications were made by manual thresholding using Qupath in vasculature lesions of 18 CTEPH patients.

© 2024 The Authors. *European Journal of Immunology* published by Wiley-VCH GmbH.

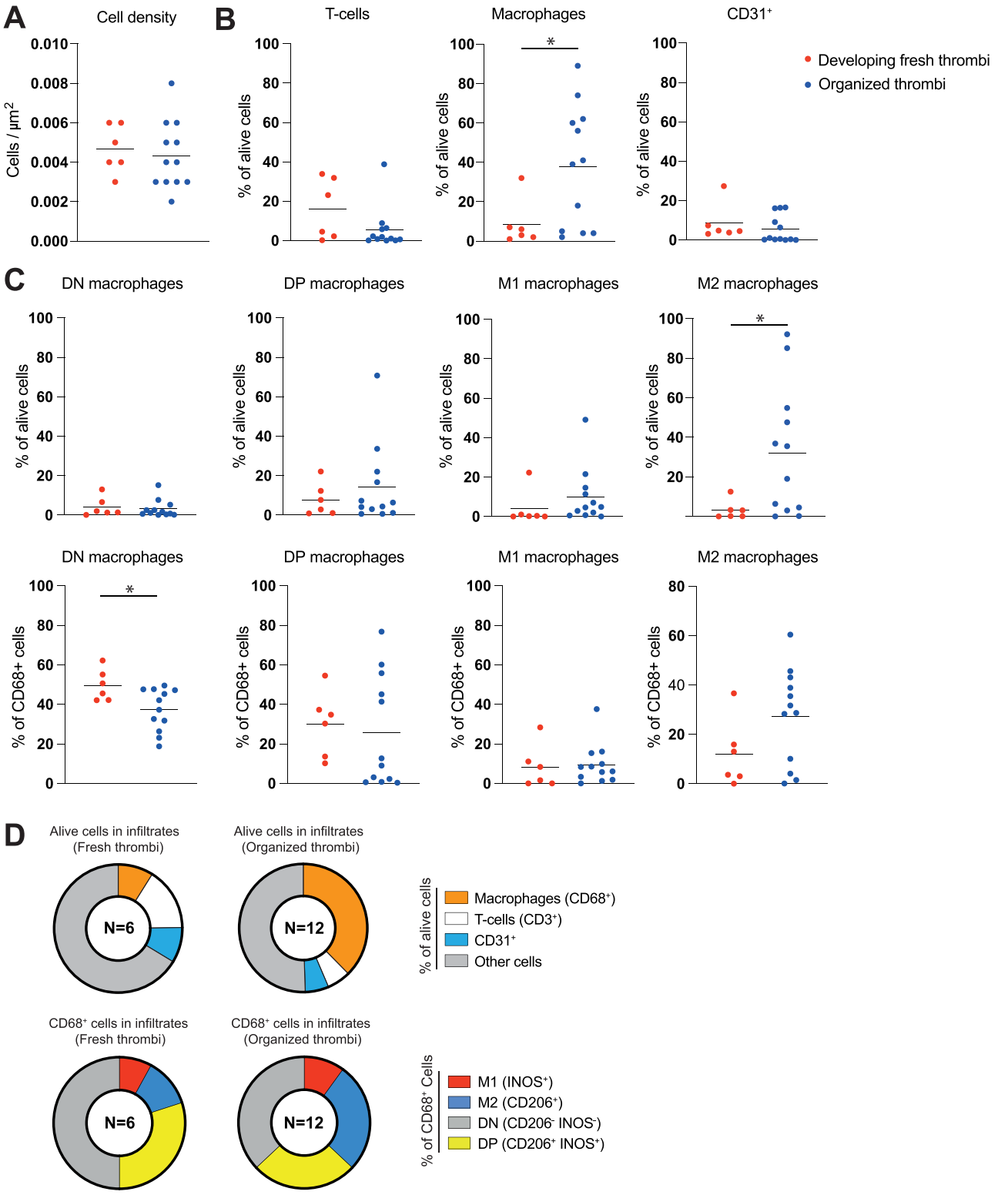

Figure 2. Shift from unpolarized macrophages in FT toward an expanded population of M2 macrophages in OT in CTEPH. Quantification of multiplex staining was conducted utilizing Qupath, an open software platform for bioimage analysis (version 0.3.0) [17]. Hematoxylin and eosin (H&E) staining was performed on serial sections to assess immune cell infiltration according to established protocols. Subsequently, these sections were annotated using specific thresholds for cell detection. The thresholds for automated 4′,6-diamidino-2-phenylindole (DAPI)-based cell detection were established through comparisons between manual H&E and automated DAPI quantifications in paired slides. Following this, automated classification and annotation of all cells were carried out based on specific marker clusters, employing thresholding for the different channels. (A) Determination of the cell density within the regions of interest, measured by Qupath software in cells/µm^2. (B) Qupath-mediated automated cell detection and quantification of the proportions of the indicated T cell (CD3$^+$), macrophage (CD68$^+$), and CD31$^+$ cell subpopulations from total

© 2024 The Authors. *European Journal of Immunology* published by Wiley-VCH GmbH.

15214141, 2024, 6, Downloaded from https://onlinelibrary.wiley.com/doi/10.1002/eji.202350670 by Erasmus University Rotterdam Universiteitsbibliotheek, Wiley Online Library on [12/06/2024]. See the Terms and Conditions (https://onlinelibrary.wiley.com/terms-and-conditions) on Wiley Online Library for rules of use; OA articles are governed by the applicable Creative Commons License

15214141, 2024, 6, Downloaded from https://onlinelibrary.wiley.com/doi/10.1002/eji.202350670 by Erasmus University Rotterdam Universiteitsbibliotheek, Wiley Online Library on [12/06/2024]. See the Terms and Conditions (https://onlinelibrary.wiley.com/terms-and-conditions) on Wiley Online Library for rules of use; OA articles are governed by the applicable Creative Commons License

experimental PH [10, 22] and in perivascular inflammatory cells in another nonthrombotic form of PH, pulmonary arterial hypertension (PAH) [23]. Furthermore, in atherosclerotic cardiovascular disease, the enrichment of M2 macrophages is thought to represent a viable strategy to promote atherosclerosis regression and plaque stabilization [24]. On the other hand, the specific presence of M2 macrophages in OT, which are characterized by a high degree of remodeling and fibrosis, would be in line with their ability to produce TGFβ and induce a profibrotic environment. The identification of M2-associated markers, such as TGFβ, IL-10, and arginase, through additional stainings further supports the notion of involvement of M2 macrophages in repair processes within this tissue. This finding underscores the complexity of macrophage polarization states and their multifaceted roles in tissue homeostasis and pathology, particularly in the context of thrombotic diseases such as CTEPH.

The M1/M2 concept, although useful in understanding tissue macrophage function in various diseases including PH, incompletely describes macrophage gene expression in vivo, considering that simultaneous expression of M1 and M2 genes was observed in tissue injury, repair, and tumor progression [25, 26]. Our finding of $CD206^{+}INOS^{+}$ DP $CD68^{+}$ macrophages in FT points to a dynamic, heterogeneous, and plastic nature of pulmonary macrophages in CTEPH. Such heterogeneity and plasticity of macrophages are clearly supported by scRNAseq studies, identifying many subclusters of alveolar macrophages in healthy human BAL fluid or macrophages in plaques of carotid artery thrombosis patients [25].

Conclusion

Although our study has limitations due to the small number of patients and the complexity of macrophage subclassification biology, we were able to find significant differences in immune cell infiltration and distribution between FT and OT. Our findings indicate differentiation from unpolarized macrophages in FT toward an expanded population of M2 macrophages in OT, pointing to a dynamic role of macrophages during CTEPH pathogenesis. Recent scRNAseq studies performed in CTEPH identified various immune cells, including macrophages, but did not subclassify them using M1 or M2 markers [27, 28]. Hereby, subclusters within the macrophage compartment were characterized by upregulated inflammatory signaling involved in pulmonary vascular remodeling. Therefore, performing further scRNAseq experiments comparing fresh and organized thrombi may offer additional insights into macrophage biology in CTEPH.

Because there is evidence for the therapeutic potential of targeting macrophages in various pulmonary diseases [5], it is attractive to explore if therapeutic strategies targeting macrophage function could be beneficial for CTEPH patients.

Materials and methods

Patient selection

PEA material, derived from our cohort of 23 CTEPH patients (Table 1), was subdivided into lesions with organized and fresh thromboembolisms, based on histologic features. Formalin-fixed paraffin-embedded (FFPE)-tissue of lung vascular lesions of CTEPH patients was handled and used according to the guidelines of the declaration of Helsinki. This study was conducted in accordance with the guidelines of the Biomedical Scientific Societies (Dutch Federal Code of Conduct 2011) for the use of anonymized residual tissue obtained during regular treatment.

Immunohistochemical multiplex staining in PEA material

We performed immunohistochemical analysis of PEA tissue, with a 5-plex immunofluorescence multiplex by automated IHC using the Ventana Benchmark Discovery ULTRA (Ventana Medical Systems Inc.), as described previously [11, 29]. Four micrometer thick FFPE sections were stained for CD3 (clone 2VG6, Ventana), CD31 (clone JC70, Ventana), INOS (polyclonal, Abcam), CD68 (clone KP1, Ventana), and CD206 (polyclonal, Sigma Aldrich). In brief, following deparaffinization and heat-induced antigen retrieval with Cell conditioning solution 1 (CC1) (#950-224, Ventana) for 32 min, anti-CD3 was incubated for 32 min at 37°C followed by omnimap anti-rabbit HRP (#760-4311, Ventana) and detection with R6G (#760-244, Ventana). An antibody denaturation step was performed with cell conditioning solution 2 (CC2; #950-123, Ventana) at 100°C for 20 min. Second, incubation with anti-CD31 was performed for 60 min at 37°C, followed by universal HQ kit (#760-275, Ventana), and detection with dicyclohexylcarbodiimide (#760-240, Ventana) for 8 min. An antibody denaturation step was followed with CC2 at 100°C for 20 min. Third, anti-CD206 was incubated for 32 min at 37°C, followed by omnimap anti-rabbit HRP (#760-4311, Ventana) and detection with Red610 (#760-245, Ventana) for 8 min. An antibody denaturation step was performed with CC2 at 100°C for 20 min. Fourth, sections were incubated with anti-INOS for 120 min at 37°C followed by universal HQ kit (#760-275, Ventana) and detection with Cy5 (#760-238, Ventana) for 8 min. An antibody denaturation step was followed with CC2 at 100°C for 20 min. Finally,

nucleated cells within the regions of interest. (C) Quantification of double negative ($CD68^{+}$ $INOS^{-}$ $CD206^{-}$), double positive ($CD68^{+}INOS^{+}CD206^{+}$), M1 ($CD68^{+}INOS^{+}$), and M2 ($CD68^{+}CD206^{+}$) macrophage subsets, as proportions of alive cells (top) or total macrophages (bottom). (D) Pie chart showing the distribution of T-cells, macrophages, $CD31^{+}$ cells, and other viable cells (top) or distribution of M1, M2, double positive (DP), and double negative macrophages (bottom). Statistical significance of data was calculated using the nonparametric Mann–Whitney *U* test. *p*-values < 0.05 were considered significant. All analyses were performed using Prism (GraphPad Software). Data are presented as scattered dot plots with mean values. CD, cluster of differentiation; INOS, inducible nitric oxide synthase. INOS; cluster of differentiation, CD; 4′,6-diamidino-2-phenylindole, DAPI.

© 2024 The Authors. *European Journal of Immunology* published by Wiley-VCH GmbH.

15214141, 2024, 6, Downloaded from https://onlinelibrary.wiley.com/doi/10.1002/eji.202350670 by Erasmus University Rotterdam Universiteitsbibliotheek, Wiley Online Library on [12/06/2024]. See the Terms and Conditions (https://onlinelibrary.wiley.com/terms-and-conditions) on Wiley Online Library for rules of use; OA articles are governed by the applicable Creative Commons License

incubation occurred with anti-CD68 for 60 min at 37°C followed by omnimap anti-rabbit HRP (#760-4311, Ventana) and detection with 6-carboxyfluorescein (FAM) (#760-243, Ventana). Finally, slides were washed in PBS and mounted with Vectashield containing 4',6-diamidino-2-phenylindole (Vector Laboratories). For additional M2 marker staining, a similar immunohistochemical analysis of PEA tissue as described above was performed, with a 5-plex immunofluorescence multiplex by automated IHC using the Ventana Benchmark Discovery ULTRA (Ventana Medical Systems Inc.), as described previously [11, 29]. Four-micrometer thick FFPE sections were stained for IL-10 (polyclonal, abcam), CD68 (clone KP1, Ventana), CD206 (polyclonal, Sigma Aldrich), TGFb (polyclonal, Abcam), and Arginase-1 (EP261, Cell Marque). In brief, following deparaffinization and heat-induced antigen retrieval with CC1 (#950-224, Ventana) for 32 min, anti-IL-10 was incubated for 40 min at 37°C followed by omnimap anti-rabbit HRP (#760-4311, Ventana) and detection with R6G (#760-244, Ventana). An antibody denaturation step was performed with CC2 (#950-123, Ventana) at 100°C for 20 min. Second, incubation with anti-CD68 was performed for 20 min at 37°C, followed by omnimap-anti-mouse HRP (#760-4310, Ventana) and detection with dicyclohexylcarbodiimide (#760-240, Ventana) for 8 min. An antibody denaturation step was followed with CC2 at 100°C for 20 min. Third, anti-CD206 was incubated for 32 min at 37°C, followed by omnimap anti-rabbit HRP (#760-4311, Ventana) and detection with Red610 (#760-245, Ventana) for 8 min. An antibody denaturation step was performed with CC2 at 100°C for 20 min. Fourth, sections were incubated with anti-TGF-beta for 32 min at 37°C followed by omnimap anti-rabbit HRP (#760-4311, Ventana) and detection with Cy5 (#760-238, Ventana) for 8 min. An antibody denaturation step was followed with CC2 at 100°C for 20 min. Lastly, incubation occurred with anti-Arginase-1 for 32 min at 37°C followed by omnimap anti-rabbit HRP (#760-4311, Ventana) and detection with 6-carboxyfluorescein (FAM) (#760-243, Ventana). Finally, slides were washed in PBS and mounted with Vectashield containing 4',6-diamidino-2-phenylindole (Vector Laboratories).

In these multiplex immunofluorescence experiments, stainings were optimized as follows: 5-plex was built by cross-validation with conventional IHC to investigate true signals, thus adjusting cut-off values for immunofluorescence signals. We also tested single IF staining of every marker to investigate the correct order of antibodies. After every primary antibody incubation, a CC2 (citrate) stripping step was performed to remove nonspecific and unbound antibodies.

Differentiation between developing FT and OT

Developing FT refers to growing blood clots that contain recently formed components and have not undergone significant organization or remodeling. These clots consist of platelets, fibrin, erythrocytes, and lymphocytes, and may coexist with areas of organized thrombus. In contrast, OT refers to older thrombi that have undergone complete remodeling. OT is characterized by the presence of fibrous tissue, neovascularization, and recanalization, without any histological evidence of recent thrombosis.

Cell detection and characterization

Slides were scanned using the Zeiss AxioImager with automatic 8-slide stage using Zen 3.2 software. Analysis of the multiplex staining was performed using Qupath, an open software platform for bioimage analysis (version 0.3.0) [17]. Serial sections were evaluated for infiltration of immune cells by H&E staining according to standard procedures and subsequently annotated using specific thresholds for cell detection. The thresholds for automated DAPI-based cell detection were determined on the basis of comparisons between manual H&E and automated DAPI quantifications in paired slides. Afterward, using thresholding for the different channels, all cells were automatically classified and annotated based on specific clusters of markers.

Acknowledgements: This research project was supported by unrestricted grants from Jansen – Cilag B.V. Pharmaceuticals and from Ferrer Pharmaceuticals.

Conflict of interest: The authors declare no financial or commercial conflict of interest.

Author contributions: Thomas Koudstaal, Jan von der Thüsen, Rudi Hendriks, and Karin Boomars designed the experiments. Thomas Koudstaal, Karin Boomars, Jan von der Thüsen, Thierry van den Bosch, Ingrid Bergen, and Rudi Hendriks performed experiments and analyzed/interpreted data. Karishma Lila and Ingrid Bergen provided valuable feedback for Qupath analyses in our manuscript. Harm Jan Bogaard and Paul Bresser provided valuable feedback for the manuscript. Thomas Koudstaal, Karin Boomars, and Rudi Hendriks wrote the manuscript, with key input from Jan von der Thüsen. All authors read and approved the final manuscript.

Ethic approval and consent to participate: All subjects gave their informed consent for inclusion before they participated in the study. The study was conducted in accordance with the Declaration of Helsinki. The samples used for our study were obtained by usage of pulmonary endarterectomy rest material, therefore approval of the ethics committee was not required for this study.

Data availability statement: The data that support the findings of this study are available from the corresponding author upon reasonable request.

Peer review: The peer review history for this article is available at https://publons.com/publon/10.1002/eji.202350670.

© 2024 The Authors. *European Journal of Immunology* published by Wiley-VCH GmbH.

References

1 **Delcroix, M., Torbicki, A., Gopalan, D., Sitbon, O., Klok, F. A., Lang, I., Jenkins, D. et al.**, ERS statement on chronic thromboembolic pulmonary hypertension. *Eur. Respir. J.* 2021. **57**: 2002828.

2 **Otani, N., Watanabe, R., Tomoe, T., Toyoda, S., Yasu, T. and Nakamoto, T.**, Pathophysiology and treatment of chronic thromboembolic pulmonary hypertension. *Int. J. Mol. Sci.* 2023. **24**: 3979.

3 **Bochenek, M., Rosinus, N., Lankeit, M., Hobohm, L., Bremmer, F., Schütz, E., Klok, F. et al.**, From thrombosis to fibrosis in chronic thromboembolic pulmonary hypertension. *Thromb. Haemost.* 2017. **117**: 769–783.

4 **Zabini, D., Heinemann, A., Foris, V., Nagaraj, C., Nierlich, P., Bálint, Z., Kwapiszewska, G. et al.**, Comprehensive analysis of inflammatory markers in chronic thromboembolic pulmonary hypertension patients. *Eur. Respir. J.* 2014. **44**: 951–962.

5 **Aegerter, H., Lambrecht, B. N. and Jakubzick, C. V.**, Biology of lung macrophages in health and disease. *Immunity* 2022. **55**: 1564–1580.

6 **Zhang, M.-Q., Wang, C.-C., Pang, X.-B., Shi, J.-Z., Li, H.-R., Xie, X.-M., Wang, Z. et al.**, Role of macrophages in pulmonary arterial hypertension. *Front. Immunol.* 2023. **14**: 1152881.

7 **Isshiki, T., Vierhout, M., Naiel, S., Ali, P., Yazdanshenas, P., Kumaran, V., Yang, Z. et al.**, Therapeutic strategies targeting pro-fibrotic macrophages in interstitial lung disease. *Biochem. Pharmacol.* 2023. **211**: 115501.

8 **Takiguchi, H., Yang, C. X., Yang, C. W. T., Sahin, B., Whalen, B. A., Milne, S., Akata, K. et al.**, Macrophages with reduced expressions of classical M1 and M2 surface markers in human bronchoalveolar lavage fluid exhibit pro-inflammatory gene signatures. *Sci. Rep.* 2021. **11**: 8282.

9 **Park, M. D., Silvin, A., Ginhoux, F. and Merad, M.**, Macrophages in health and disease. *Cell* 2022. **185**: 4259–4279.

10 **Zawia, A., Arnold, N. D., West, L., Pickworth, J. A., Turton, H., Iremonger, J., Braithwaite, A. T. et al.**, Altered macrophage polarization induces experimental pulmonary hypertension and is observed in patients with pulmonary arterial hypertension. *Arterioscler. Thromb. Vasc. Biol.* 2021. **41**: 430–445.

11 **Van Uden, D., Koudstaal, T., Van Hulst, J. A. C., Van Den Bosch, T. P. P., Vink, M., Bergen, I. M., Lila, K. A. et al.**, Evidence for a role of CCR6+ T cells in chronic thromboembolic pulmonary hypertension. *Front. Immunol.* 2022. **13**: 861450.

12 **Wasilko, D. J., Johnson, Z. L., Ammirati, M., Che, Y., Griffor, M. C., Han, S. and Wu, H.**, Structural basis for chemokine receptor CCR6 activation by the endogenous protein ligand CCL20. *Nat. Commun.* 2020. **11**: 3031.

13 **Tesmer, L. A., Lundy, S. K., Sarkar, S. and Fox, D. A.**, Th17 cells in human disease. *Immunol. Rev.* 2008. **223**: 87–113.

14 **Bazzan, E., Turato, G., Tinè, M., Radu, C. M., Balestro, E., Rigobello, C., Biondini, D. et al.**, Dual polarization of human alveolar macrophages progressively increases with smoking and COPD severity. *Respir. Res.* 2017. **18**: 40.

15 **Heo, J. H., Nam, H. S., Kim, Y. D., Choi, J. K., Kim, B. M., Kim, D. J. and Kwon, I.**, Pathophysiologic and therapeutic perspectives based on thrombus histology in stroke. *J. Stroke* 2020. **22**: 64–75.

16 **Lin, P., Ji, H.-H., Li, Y.-J. and Guo, S.-D.**, Macrophage plasticity and atherosclerosis therapy. *Front. Mol. Biosci.* 2021. **8**: 679797.

17 **Bankhead, P., Loughrey, M. B., Fernández, J. A., Dombrowski, Y., Mcart, D. G., Dunne, P. D., Mcquaid, S. et al.**, QuPath: open source software for digital pathology image analysis. *Sci. Rep.* 2017. **7**: 16878.

18 **Akata, K., Yamasaki, K., Leitao Filho, F. S., Yang, C. X., Takiguchi, H., Sahin, B., Whalen, B. A. et al.**, Abundance of non-polarized lung macrophages with poor phagocytic function in chronic obstructive pulmonary disease (COPD). *Biomedicines* 2020. **8**: 398.

19 **Draijer, C., Florez-Sampedro, L., Reker-Smit, C., Post, E., Van Dijk, F. and Melgert, B. N.**, Explaining the polarized macrophage pool during murine allergic lung inflammation. *Front. Immunol.* 2022. **13**: 1056477.

20 **Martinez, F. O., Helming, L. and Gordon, S.**, Alternative activation of macrophages: an immunologic functional perspective. *Annu. Rev. Immunol.* 2009. **27**: 451–483.

21 **Zhang, L., Wang, Y., Wu, G., Xiong, W., Gu, W. and Wang, C.-Y.**, Macrophages: friend or foe in idiopathic pulmonary fibrosis? *Respir. Res.* 2018. **19**: 170.

22 **Fan, Y., Hao, Y., Gao, D., Li, G. and Zhang, Z.**, Phenotype and function of macrophage polarization in monocrotaline-induced pulmonary arterial hypertension rat model. *Physiol. Res.* 2021. **70**: 213–226.

23 **Savai, R., Pullamsetti, S. S., Kolbe, J., Bieniek, E., Voswinckel, R., Fink, L., Scheed, A. et al.**, Immune and inflammatory cell involvement in the pathology of idiopathic pulmonary arterial hypertension. *Am J. Respir. Crit. Care Med.* 2012. **186**: 897–908.

24 **Barrett, T. J.**, Macrophages in atherosclerosis regression. *Arterioscler. Thromb. Vasc. Biol.* 2020. **40**: 20–33.

25 **Fernandez, D. M., Rahman, A. H., Fernandez, N. F., Chudnovskiy, A., Amir, E.-A. D., Amadori, L., Khan, N. S. et al.**, Single-cell immune landscape of human atherosclerotic plaques. *Nat. Med.* 2019. **25**: 1576–1588.

26 **Xue, J., Schmidt, S. V., Sander, J., Draffehn, A., Krebs, W., Quester, I., De Nardo, D. et al.**, Transcriptome-based network analysis reveals a spectrum model of human macrophage activation. *Immunity* 2014. **40**: 274–288.

27 **Miao, R., Dong, X., Gong, J., Li, Y., Guo, X., Wang, J., Huang, Q. et al.**, Examining the development of chronic thromboembolic pulmonary hypertension at the single-cell level. *Hypertension* 2022. **79**: 562–574.

28 **Viswanathan, G., Kirshner, H. F., Nazo, N., Ali, S., Ganapathi, A., Cumming, I., Zhuang, Y. et al.**, Single-cell analysis reveals distinct immune and smooth muscle cell populations that contribute to chronic thromboembolic pulmonary hypertension. *Am J. Respir. Crit. Care Med.* 2023. **207**: 1358–1375.

29 **Zhang, W., Hubbard, A., Jones, T., Racolta, A., Bhaumik, S., Cummins, N., Zhang, L. et al.**, Fully automated 5-plex fluorescent immunohistochemistry with tyramide signal amplification and same species antibodies. *Lab. Invest.* 2017. **97**: 873–885.

Abbreviations: **BPA**: balloon pulmonary angioplasty · **CC2**: cell conditioning solution 2 · **CTEPH**: chronic thromboembolic pulmonary hypertension · **DAPI**: 4′,6-diamidino-2-phenylindole · **DN**: double negative · **DP**: double positive · **FFPE**: formalin-fixed paraffin-embedded · **FT**: fresh thrombi · **iNOS**: inducible nitric oxide synthase · **MCP-1**: monocyte chemoattractant protein-1 · **MIP-1α**: macrophage inflammatory protein-1α · **OT**: organized thrombi · **PEA**: pulmonary endarterectomy · **PH**: pulmonary hypertension · **scRNAseq**: single-cell RNA sequencing

Full correspondence: Dr. Thomas Koudstaal, Department of Pulmonary Medicine, Erasmus MC, University Medical Center Rotterdam, Dr Molenwaterplein 40, 3015GD Rotterdam, The Netherlands
e-mail: t.koudstaal.1@erasmusmc.nl

Received: 15/7/2023
Revised: 14/3/2024
Accepted: 18/3/2024
Accepted article online: 22/3/2024

© 2024 The Authors. *European Journal of Immunology* published by Wiley-VCH GmbH.

15214141, 2024, 6, Downloaded from https://onlinelibrary.wiley.com/doi/10.1002/eji.202350670 by Erasmus University Rotterdam Universiteitsbibliotheek, Wiley Online Library on [12/06/2024]. See the Terms and Conditions (https://onlinelibrary.wiley.com/terms-and-conditions) on Wiley Online Library for rules of use; OA articles are governed by the applicable Creative Commons License